

# Loss of XL $\alpha$ s (extra-large $\alpha$ s) imprinting results in early postnatal hypoglycemia and lethality in a mouse model of pseudohypoparathyroidism Ib

Eduardo Fernández-Rebollo<sup>a,1</sup>, Akira Maeda<sup>a</sup>, Monica Reyes<sup>a</sup>, Serap Turan<sup>a,b</sup>, Leopold F. Fröhlich<sup>a,c</sup>, Antonius Plagge<sup>d</sup>, Gavin Kelsey<sup>e,f</sup>, Harald Jüppner<sup>a,g</sup>, and Murat Bastepe<sup>a,2</sup>

<sup>a</sup>Endocrine Unit, Department of Medicine, and <sup>9</sup>Pediatric Nephrology, Massachusetts General Hospital and Harvard Medical School, Boston, MA 02114; <sup>b</sup>Pediatric Endocrinology, Marmara University School of Medicine, Istanbul 34899, Turkey; <sup>c</sup>Institute of Pathology, Medical University of Graz, 8036 Graz, Austria; <sup>d</sup>Cellular and Molecular Physiology, Institute of Translational Medicine, University of Liverpool, Liverpool L69 3BX, United Kingdom; <sup>e</sup>Epigenetics Programme, The Babraham Institute, Cambridge CB22 3AT, United Kingdom; and <sup>f</sup>Centre for Trophoblast Research, University of Cambridge, Cambridge CB2 1TN, United Kingdom

Edited\* by John T. Potts, Massachusetts General Hospital, Charlestown, MA, and approved March 19, 2012 (received for review October 25, 2011)

**Maternal deletion of the NESP55 differentially methylated region (DMR) (delNESP55/ASdel3-4<sup>m</sup>, delINAS<sup>m</sup>) from the GNAS locus in humans causes autosomal dominant pseudohypoparathyroidism type Ib (AD-PHP-Ib<sup>delINAS<sup>m</sup></sup>), a disorder of proximal tubular parathyroid hormone (PTH) resistance associated with loss of maternal GNAS methylation imprints. Mice carrying a similar, maternally inherited deletion of the Nesp55 DMR ( $\Delta$ Nesp55<sup>m</sup>) replicate these Gnas epigenetic abnormalities and show evidence for PTH resistance, yet these mice demonstrate 100% mortality during the early postnatal period. We investigated whether the loss of extra-large  $\alpha$ s (XL $\alpha$ s) imprinting and the resultant biallelic expression of XL $\alpha$ s are responsible for the early postnatal lethality in  $\Delta$ Nesp55<sup>m</sup> mice. First, we found that  $\Delta$ Nesp55<sup>m</sup> mice are hypoglycemic and have reduced stomach-to-body weight ratio. We then generated mice having the same epigenetic abnormalities as the  $\Delta$ Nesp55<sup>m</sup> mice but with normalized XL $\alpha$ s expression due to the paternal disruption of the exon giving rise to this Gnas product. These mice ( $\Delta$ Nesp55<sup>m</sup>/Gnas<sup>l<sup>m+/p-</sup></sup>) showed nearly 100% survival up to postnatal day 10, and a substantial number of them lived to adulthood. The hypoglycemia and reduced stomach-to-body weight ratio observed in 2-d-old  $\Delta$ Nesp55<sup>m</sup> mice were rescued in the  $\Delta$ Nesp55<sup>m</sup>/Gnas<sup>l<sup>m+/p-</sup></sup> mice. Surviving double-mutant animals had significantly reduced G $\alpha$ s mRNA levels and showed hypocalcemia, hyperphosphatemia, and elevated PTH levels, thus providing a viable model of human AD-PHP-Ib. Our findings show that the hypoglycemia and early postnatal lethality caused by the maternal deletion of the Nesp55 DMR result from biallelic XL $\alpha$ s expression. The double-mutant mice will help elucidate the pathophysiological mechanisms underlying AD-PHP-Ib.**

stimulatory G protein | renal proximal tubule | cyclic AMP

**M**ost autosomal genes are expressed equally from both parental alleles, but in a subset of mammalian genes, the transcription from one allele is epigenetically repressed based on its parent of origin; this process is called genomic imprinting (1, 2). The proper dosage of imprinted genes is critical for survival, and aberrant expression of normally imprinted alleles is responsible for several human disorders, including, but not limited to, Beckwith–Wiedemann syndrome [Mendelian Inheritance in Man (MIM) 130650], Prader–Willi syndrome (MIM 176270), Angelman syndrome (MIM 105830), Silver–Russell syndrome (MIM 180860), transient neonatal diabetes (MIM 601410), and autosomal dominant pseudohypoparathyroidism type Ib (AD-PHP-Ib; MIM 603233).

The genes encoding human and mouse G $\alpha$ s (GNAS and Gnas) are complex, imprinted loci located within chromosomal regions of conserved synteny (distal chromosome 2 in mice, 20q13.32 in humans) and have similar overall organizations (3–5). GNAS/Gnas generates multiple gene products through the use of

different alternative promoters and first exons that splice onto common exons (2–13 in humans and 2–12 in mice) (Fig. S1). The most downstream alternative first exon is G $\alpha$ s exon 1, which generates transcripts encoding the ubiquitously expressed G $\alpha$ s (6). The G $\alpha$ s promoter resides within a nonmethylated CpG island, but despite the absence of differential methylation at its promoter, G $\alpha$ s shows predominantly maternal expression in some tissues, including pituitary, thyroid, renal proximal tubules, and gonads (7–10); G $\alpha$ s expression is biallelic in most other tissues (11–13). The furthest upstream alternative promoter generates transcripts that encode the neuroendocrine-specific protein of 55 kDa (NESP55; mouse Nesp55), a chromogranin-like protein, the coding sequence of which is located within a specific upstream exon; G $\alpha$ s exons 2–13 reside within the 3' untranslated region of NESP55 transcripts (14). This mRNA shows exclusive maternal expression, because its promoter is methylated on the paternal allele (12, 15, 16). A third alternative promoter generates transcripts encoding the extralarge G $\alpha$ s isoform (XL $\alpha$ s) (17). XL $\alpha$ s has a long amino-terminal extension encoded by its specific first exon, whereas the remainder of the protein is identical to G $\alpha$ s. XL $\alpha$ s is imprinted oppositely to NESP55; i.e., its promoter is methylated on the maternal allele and transcriptionally active only on the paternal allele (12, 15, 16). Within the same differentially methylated region (DMR) and just upstream of the XL $\alpha$ s promoter is a promoter driving expression of a paternally expressed antisense transcript, which is noncoding and traverses the NESP55 exon from the opposite direction (AS; mouse Nespas) (18, 19). Like XL $\alpha$ s, this AS transcript is expressed from the paternal allele. A fifth alternative promoter and first exon (A/B; mouse exon 1A) also splices onto exons 2–13 (mouse 2–12) (20). The A/B transcript is paternally expressed and presumed to be untranslated (21), although a recent study has shown that it can lead to an amino-terminally truncated G $\alpha$ s variant that may have biological activity (22).

Loss of methylation at the maternal A/B exon and promoter leading to biallelic A/B expression is found in patients with PHP-Ib, who show renal parathyroid hormone (PTH) resistance presumably due to G $\alpha$ s deficiency in the renal proximal tubule

Author contributions: E.F.-R., H.J., and M.B. designed research; E.F.-R., A.M., M.R., and S.T. performed research; L.F.F., A.P., and G.K. contributed new reagents/analytic tools; E.F.-R., A.M., H.J., and M.B. analyzed data; and E.F.-R., H.J., and M.B. wrote the paper.

The authors declare no conflict of interest.

\*This Direct Submission article had a prearranged editor.

<sup>1</sup>Present address: Diabetes and Obesity Laboratory, Endocrinology and Nutrition Unit, Institut d'Investigacions Biomediques August Pi i Sunyer, Hospital Clinic de Barcelona, 08028 Barcelona, Spain.

<sup>2</sup>To whom correspondence should be addressed. E-mail: bastepe@helix.mgh.harvard.edu.

This article contains supporting information online at [www.pnas.org/lookup/suppl/doi:10.1073/pnas.1117608109/-DCSupplemental](http://www.pnas.org/lookup/suppl/doi:10.1073/pnas.1117608109/-DCSupplemental).

(23, 24). This finding suggests that exon A/B controls tissue-specific *Gas* imprinting via the presence of one or more regulatory *cis*-acting elements that are both tissue-specific and methylation-sensitive. Genetic microdeletions identified in AD-PHP-1b suggest that *cis*-acting elements within the nearby *STX16* locus and the upstream NESP55 DMR or transcription from the NESP55 promoter may be critical for the establishment and/or maintenance of exon A/B maternal-specific methylation (25–29).

We recently developed a mouse model of AD-PHP-1b by deleting the maternal Nesp55 DMR (30) in a manner similar to the deletions described in some patients with this disease (26). This mouse strain,  $\Delta$ Nesp55<sup>tm</sup>, phenocopies AD-PHP-1b with respect to the *GNAS* imprinting defects—i.e., loss of all of the maternal *Gnas* methylation imprints combined with increased (biallelic) 1A transcription—and with respect to the abnormal regulation of mineral ion homeostasis—i.e., hypocalcemia, hyperphosphatemia, and secondary hyperparathyroidism (30). However, unlike the findings in patients with deletions involving NESP55 and antisense exons 3 and 4 (AD-PHP-1b<sup>delINAS5m</sup>), there is 100% early postnatal lethality in  $\Delta$ Nesp55<sup>tm</sup> mice, whereas mice in which the paternal Nesp55 DMR is deleted ( $\Delta$ Nesp55<sup>p</sup> mice) show no epigenetic and biochemical abnormalities and have an apparently normal phenotype and life span. The lethality in  $\Delta$ Nesp55<sup>tm</sup> mice, which was assumed to reflect worsening hypocalcemia during the first 5 d of life, prevented additional investigation of this mouse model of AD-PHP-1b regarding the mechanisms underlying PTH resistance.

In this study, we further investigated the cause of the early postnatal death in  $\Delta$ Nesp55<sup>tm</sup> mice to reach a better understanding of the consequences of abnormal *Gnas* methylation and, thereby, to generate hypotheses as to how to extend the life span of this AD-PHP-1b mouse model. Both 1A and XL $\alpha$ s transcripts are expressed biallelically in these mice. Biological roles of the XL $\alpha$ s protein remain almost completely unknown, but data from mouse models have shown that it is essential for postnatal adaptation to feeding and for glucose and energy metabolism. Moreover, some *in vivo* data indicate that XL $\alpha$ s can oppose the actions of *Gas* (31–33). We therefore reasoned that overexpression of XL $\alpha$ s contributes to the phenotype in the  $\Delta$ Nesp55<sup>tm</sup> mice by further antagonizing the already diminished *Gas* actions. For example, hypocalcemia associated with lowered *Gas* levels in the kidney, and the resultant PTH resistance, could be exacerbated by increased XL $\alpha$ s levels. To address whether the loss of XL $\alpha$ s imprinting is involved in the phenotypes observed in the  $\Delta$ Nesp55<sup>tm</sup> mice, we generated mice in which the *Gnas* methylation profile of the  $\Delta$ Nesp55<sup>tm</sup> mice is preserved but the expression of XL $\alpha$ s is confined to a single parental allele. Our investigations revealed that the loss of XL $\alpha$ s imprinting contributes significantly to the early postnatal lethality phenotype observed in  $\Delta$ Nesp55<sup>tm</sup> mice.

## Results

The  $\Delta$ Nesp55<sup>tm</sup> mice die within 5 d of postnatal life in 129/S2 and C57BL/6J backgrounds (30). As an attempt to improve survival of these mice, we crossed them into the outbred CD1 strain, but the early postnatal lethality did not change significantly, with no pups surviving until postnatal day 10 (P10). We have previously shown that  $\Delta$ Nesp55<sup>tm</sup> mice are hypocalcemic at P2 and attributed the lethality to the possible worsening of the low calcium levels by day 5 (30). To determine whether other factors could underlie or contribute to the early postnatal lethality of the  $\Delta$ Nesp55<sup>tm</sup> mice, we measured blood glucose levels at P2. Compared with wild-type littermates,  $\Delta$ Nesp55<sup>tm</sup> pups were hypoglycemic [ $81.8 \pm 5.0$  mg/dL ( $n = 21$ ) vs.  $54.0 \pm 4.0$  mg/dL ( $n = 28$ );  $P < 0.05$ ] and had considerably lower, albeit readily measureable, insulin levels (Fig. S2). Corticosterone levels were markedly higher than in wild-type littermates (Fig. S2), thus ruling out adrenal insufficiency as the cause of hypoglycemia. Most  $\Delta$ Nesp55<sup>tm</sup> mice had visible milk in

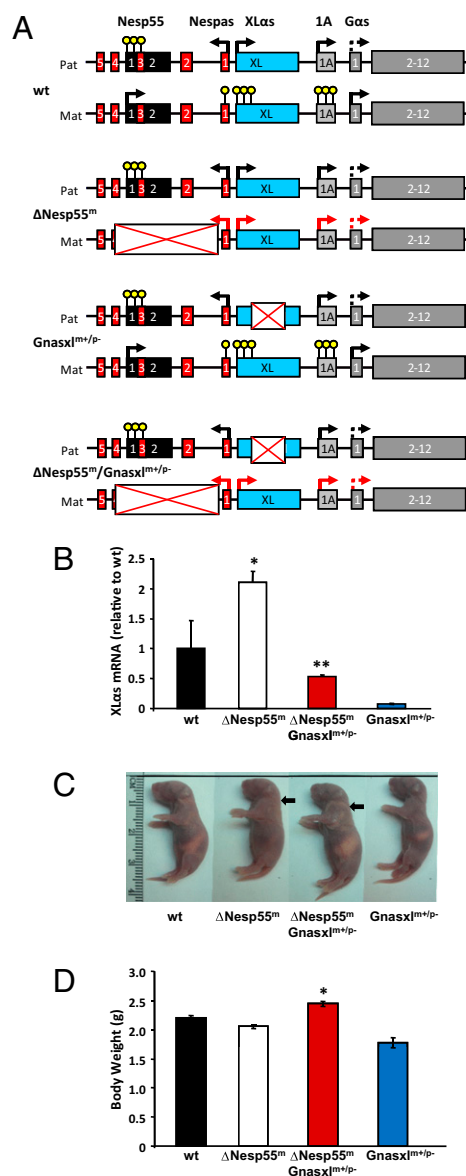


**Fig. 1.** Generation of the double-mutant  $\Delta$ Nesp55<sup>tm</sup>/Gnasxl<sup>mm+/p-</sup> mice. (A) Schematic representation of the imprinted mouse *Gnas* locus in wild-type (wt) mice and the changes induced by the deletions of Nesp55 ( $\Delta$ Nesp55<sup>tm</sup>) and XL $\alpha$ s (Gnasxl<sup>mm+/p-</sup>); introns, lines; exons, rectangles; methylated DMRs, yellow circles; transcriptional start site and direction, black arrows. Tissue-specific paternal silencing of *Gas* is indicated by a dotted arrow, and repressed promoters due to the inserted deletion (white rectangle with a red cross) by red arrows. (B) XL $\alpha$ s mRNA expression levels as determined by qRT-PCR using total RNA from whole kidneys of 2-d-old wild-type (wt),  $\Delta$ Nesp55<sup>tm</sup>,  $\Delta$ Nesp55<sup>tm</sup>/Gnasxl<sup>mm+/p-</sup>, and Gnasxl<sup>mm+/p-</sup> pups. Levels were normalized to  $\beta$ -actin mRNA and are shown relative to the expression levels in wild-type mice; data are mean  $\pm$  SEM ( $n = 3$  or 4 mice per genotype). \* $P < 0.05$  compared with wild type; \*\*not statistically significant vs. wild type and  $P < 0.01$  vs.  $\Delta$ Nesp55<sup>tm</sup>. (C) Photographs of 2-d-old mice of each genotype; note the low amount of milk in the stomach of  $\Delta$ Nesp55<sup>tm</sup> mice. Arrows point to the edema observed in  $\Delta$ Nesp55<sup>tm</sup> and  $\Delta$ Nesp55<sup>tm</sup>/Gnasxl<sup>mm+/p-</sup> mice. (D) Body weights of 2-d-old mice. \* $P < 0.001$  vs.  $\Delta$ Nesp55<sup>tm</sup> and Gnasxl<sup>mm+/p-</sup>.

their stomach, but compared with wild-type littermates, there was a ~50% reduction in their stomach-to-body weight ratio [ $0.0572 \pm 0.0034$  ( $n = 10$ ) vs.  $0.0278 \pm 0.0026$  ( $n = 20$ );  $P < 0.05$ ], an indirect measure that has previously been used to assess food intake (31). Thus, these results indicated that  $\Delta$ Nesp55<sup>tm</sup> pups were feeding insufficiently.

To determine whether the loss of XL $\alpha$ s imprinting and the consequently doubled XL $\alpha$ s expression level could underlie any of these early postnatal phenotypes in the  $\Delta$ Nesp55<sup>tm</sup> mice, we mated female  $\Delta$ Nesp55<sup>P</sup> mice with male  $Gnasxl^{m+/p-}$  or  $Gnasxl^{m-/p+}$  mice, which resulted in four genotypes, including double mutants ( $\Delta$ Nesp55<sup>tm</sup>/ $Gnasxl^{m+/p}$ ), in which paternal XL $\alpha$ s expression was abolished and maternal XL $\alpha$ s expression was derepressed (Fig. 1A). Consistent with this reestablished mono-allelic expression, the level of XL $\alpha$ s mRNA was normalized in the double-mutant offspring, as judged by quantitative RT-PCR (qRT-PCR) experiments using total RNA from whole kidneys of 2-d-old mice (Fig. 1B). As expected from findings in  $Gnasxl^{m+/p-}$  mice (31), the  $Gnas$  methylation status in  $\Delta$ Nesp55<sup>tm</sup>/ $Gnasxl^{m+/p-}$  pups was identical to that of  $\Delta$ Nesp55<sup>tm</sup>, showing a loss of all of the maternal imprints and an apparent gain of methylation at Nesp55 (Fig. S3).

Subcutaneous edema noted in early postnatal  $\Delta$ Nesp55<sup>tm</sup> pups (30) also existed in  $\Delta$ Nesp55<sup>tm</sup>/ $Gnasxl^{m+/p-}$  littermates (Fig. 1C). However, the latter animals were visibly bigger (Fig. 1C) and weighed significantly more at P2 (Fig. 1D) than both  $\Delta$ Nesp55<sup>tm</sup> and  $Gnasxl^{m+/p-}$  littermates. At this age, approximately equal numbers of pups of each genotype were alive (Table 1). Two-day-old double-mutant mice had normal blood glucose levels, unlike their  $\Delta$ Nesp55<sup>tm</sup> or  $Gnasxl^{m+/p-}$  littermates, which were both hypoglycemic (Fig. 2A). During a 3-h fasting period, wild-type and double-mutant mice displayed a similar blood glucose profile;  $\Delta$ Nesp55<sup>tm</sup> or  $Gnasxl^{m+/p-}$  showed much lower blood glucose levels at baseline than wild-type and double-mutant mice; all strains, with the exception of  $\Delta$ Nesp55<sup>tm</sup> mice, showed a drop in the levels within the first hour, which was followed by a rise to the initial values by the second hour (Fig. 2B). Only  $\Delta$ Nesp55<sup>tm</sup> mice seemed to maintain constant glucose levels during fasting (Fig. 2B). In  $Gnasxl^{m+/p-}$  pups, however, the blood glucose level diminished in the first hour, but no recovery to the initial value was observed, with the hypoglycemia after 3 h being more severe than that observed before fasting (Fig. 2B). The  $\Delta$ Nesp55<sup>tm</sup>/ $Gnasxl^{m+/p-}$  and wild-type littermates had similar stomach weights, unlike  $\Delta$ Nesp55<sup>tm</sup> and  $Gnasxl^{m+/p-}$  littermates, which both showed a similar degree of reduction in stomach weight (Fig. 2C). Consistent with inadequate feeding,  $\Delta$ Nesp55<sup>tm</sup> and  $Gnasxl^{m+/p-}$  pups had significantly lower liver glycogen content than double-mutant and wild-type littermates (Fig. 2D).

At P10, no  $\Delta$ Nesp55<sup>tm</sup> mice were found alive. In contrast, double-mutant littermates were observed at a frequency close to that predicted from Mendelian inheritance, although the number of surviving  $\Delta$ Nesp55<sup>tm</sup>/ $Gnasxl^{m+/p-}$  was slightly lower than wild-type littermates (Table 1). These results indicated a marked improvement in the survival of double-mutant mice compared with  $\Delta$ Nesp55<sup>tm</sup> mice. The 10-d-old  $\Delta$ Nesp55<sup>tm</sup>/ $Gnasxl^{m+/p-}$  mice weighed significantly less than wild-type littermates ( $6.62 \pm 0.64$  vs.  $8.60 \pm 0.25$  g;  $n = 10$ ;  $P < 0.05$ ) and were significantly hypocalcemic (Fig. 3A). The mean plasma phosphorus and PTH levels in 10-d-old  $\Delta$ Nesp55<sup>tm</sup>/ $Gnasxl^{m+/p-}$  mice tended to be higher than wild-type littermates, although statistical significance could not be reached (Fig. 3B and C). Interestingly, 10-d-old

$Gnasxl^{m+/p-}$  littermates also showed mild but significant hypocalcemia, combined with hyperphosphatemia (Fig. 3A and B).

Despite the markedly improved survival during the early postnatal period, many of the double-mutant mice died between day 10 and weaning, but a small number lived to adulthood (Table 1). The number of surviving  $\Delta$ Nesp55<sup>tm</sup>/ $Gnasxl^{m+/p-}$  adults, however, was sufficient for further investigations with respect to the actions of PTH. These mice were hypocalcemic and hyperphosphatemic and had plasma PTH levels that tended to be higher than wild-type littermates (Fig. 3D–F). Consistent with these findings, qRT-PCR experiments showed that  $G\alpha s$  mRNA levels in the proximal renal tubules of adult double mutants were ~50% lower than that in wild-type littermates (Fig. 4A). Upon exogenous PTH administration (50 nmol/kg s.c.), wild-type mice showed a robust increase in urinary cAMP levels, whereas the double-mutant mice had a significantly blunted response (Fig. 4B). The elevation of plasma cAMP in response to PTH administration was also blunted in  $\Delta$ Nesp55<sup>tm</sup>/ $Gnasxl^{m+/p-}$  mice (Fig. S4). However, PTH administration led to a marked increase in blood-ionized calcium in both  $\Delta$ Nesp55<sup>tm</sup>/ $Gnasxl^{m+/p-}$  mice and wild-type littermates (Fig. 4C). Surprisingly,  $Gnasxl^{m+/p-}$  mice failed to show a significant calcemic response to PTH (Fig. 4C).

## Discussion

We have previously generated mice in which the  $Gnas$  Nesp55 DMR was ablated (30). Maternal deletion of this DMR led to a loss of all maternal  $Gnas$  imprint marks and biochemical abnormalities consistent with PTH resistance, similar to that observed in AD-PHP-Ib<sup>delINASm</sup> patients, who carry the equivalent deletion in the same locus. Loss of A/B imprinting is thought to silence, in a tissue-specific manner, the downstream  $G\alpha s$  promoter *in cis*, thereby reducing  $G\alpha s$  expression levels and leading to PTH resistance. Because  $\Delta$ Nesp55<sup>tm</sup> mice, unlike patients with AD-PHP-Ib<sup>delINASm</sup>, showed 100% early postnatal lethality, we further investigated these mice to search for the cause of this unexpected phenotype. The  $\Delta$ Nesp55<sup>tm</sup> mice show loss of XL $\alpha$ s imprinting (30), and we therefore asked whether the early postnatal phenotype of the  $\Delta$ Nesp55<sup>tm</sup> mice resulted from the loss of XL $\alpha$ s imprinting. Our findings revealed that  $\Delta$ Nesp55<sup>tm</sup> mice are hypoglycemic and that this phenotype, as well as the early postnatal demise of these animals, can be prevented by normalizing XL $\alpha$ s expression. These observations indicate that restricting the expression of XL $\alpha$ s (or any of the other  $Gnas$  products that use exon XL, e.g., XL $\alpha$ s-N1, XXL $\alpha$ s, and ALEX; refs. 34–37) to a single parental allele is critical for survival and maintaining normal blood glucose levels during the early postnatal period.

Based on stomach-to-body weight ratios, 2-d-old  $\Delta$ Nesp55<sup>tm</sup> mice, like  $Gnasxl^{m+/p-}$  mice (31), do not have sufficient milk intake. It thus appears that both XL $\alpha$ s deficiency and XL $\alpha$ s excess lead to poor postnatal adaptation to feeding. In  $Gnasxl^{m+/p-}$  mice, a feeding defect was proposed based on the lack of XL $\alpha$ s expression in the nuclei innervating the orofacial muscles and the tongue (31). It is conceivable that XL $\alpha$ s excess also impairs

**Table 1. Frequency of each genotype among offspring from  $\Delta$ Nesp55<sup>tm</sup> and  $Gnasxl^{m+/p-}$  intercrosses**

Age	Wild type, n (%)	$\Delta$ Nesp55 <sup>tm</sup> , n (%)	$\Delta$ Nesp55 <sup>tm</sup> / $Gnasxl^{m+/p-}$ , n (%)	$Gnasxl^{m+/p-}$ , n (%)	Total born
P2	56 (23.9)	50 (21.4)	50 (21.4)	54 (23.1)	234
P10	41 (25.3)	0 (0)	36 (22.2)*	31 (19.1)**	162
Adult	33 (26.6)	0 (0)	9 (7.3)	16 (12.9)	124

The values represent the number of surviving pups and percentage (in parentheses) relative to the total number of pups that were born. Data were obtained from 18, 12, and 10 litters for P2, P10, and adult mice, respectively. Number of dead pups for individual genotypes was estimated according to the number of wild-type pups, assuming 100% survival for the latter. \* $P < 0.05$ ; \*\* $P < 0.001$  compared with wild type by  $\chi^2$  analysis using live and dead animals.

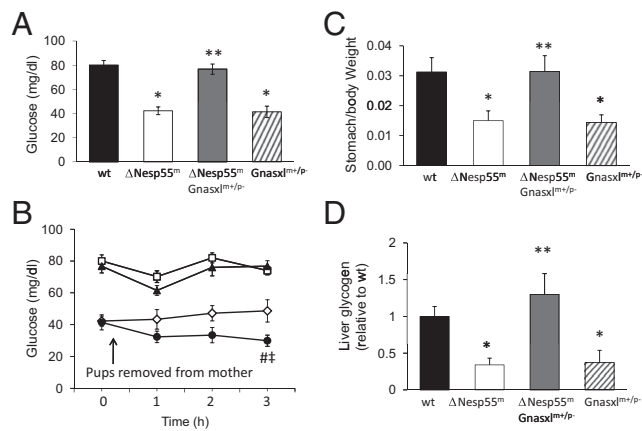


**Fig. 2.** Glucose, food intake, and liver glycogen content in 2-d-old pups. (A) Blood glucose levels in different genotypes. (B) Blood glucose levels during 3-h fasting period in wild-type (wt;  $\square$ ),  $\Delta Nesp55^m$  ( $\diamond$ ),  $\Delta Nesp55^m/Gnasxl^{m+/p-}$  ( $\blacktriangle$ ), and  $Gnasxl^{m+/p-}$  ( $\bullet$ ) mice. (C) Stomach-to-body weight ratio. (D) Liver glycogen content. Data are expressed as mean  $\pm$  SEM ( $n = 16$ –23 per genotype for basal glucose;  $n = 4$ –12 per genotype for fasting glucose;  $n = 13$ –16 per genotype for stomach-to-body weight ratio;  $n = 5$ –11 per genotype for glycogen). \* $P < 0.05$  vs. wild type; \*\* $P < 0.05$  vs.  $\Delta Nesp55^m$  and  $Gnasxl^{m+/p-}$ ; # $P < 0.005$  vs. wild type,  $\Delta Nesp55^m/Gnasxl^{m+/p-}$ , and  $\Delta Nesp55^m$ ;  $^{\ddagger}P < 0.05$  vs. 0 h.

innervations of these sites and, thereby, leads to a feeding defect through a related mechanism. Alternatively, the feeding difficulty in  $\Delta Nesp55^m$  mice can result from a generalized neurological or motor defect that prevents the pups from getting access to the mother. In fact, some of the  $\Delta Nesp55^m$  pups appear hyperactive (30), which may reflect a neurological defect.

The poor feeding and the depletion of liver glycogen likely contribute to the hypoglycemia observed in  $\Delta Nesp55^m$  mice and their  $Gnasxl^{m+/p-}$  littermates. Interestingly, however, our analysis of  $Gnasxl^{m+/p-}$  pups at P2 revealed a fasting glucose profile that is consistent with a defect in glucose counterregulation. Such a defect has been suggested for  $Gnasxl^{m+/p-}$  mice based on inappropriately low glucagon and inappropriately normal epinephrine, norepinephrine, and corticosterone levels (31). Some  $Gnasxl^{m+/p-}$  mice, despite having apparently defective glucose counterregulation, are able to survive in the outbred CD1 mouse strain (31), whereas no  $\Delta Nesp55^m$  mice are rescued by crossing into different strains (30). Thus, mechanisms other than hypoglycemia likely contribute to the early postnatal lethality in the

$\Delta Nesp55^m$  mice. Nonetheless, our findings show that the survival of these mice is markedly improved by limiting XL $\alpha$ s expression to a single allele. This finding accords with observations made in mice with disruption of Nesp55 transcription ( $Nesp55^{trun}$ ), in which there is variable loss of methylation of the XL $\alpha$ s and A/B DMRs (29). Mice with loss of methylation of both DMRs, and therefore with overexpression of XL $\alpha$ s, die within a few days of birth. In contrast, survival to weaning is observed in some mice with loss of methylation restricted to the A/B DMRs, which retain normal XL $\alpha$ s expression from only the paternal allele. Thus, the mechanism leading to the early postnatal lethality in  $\Delta Nesp55^m$  mice remains to be investigated. Availability of mice in which XL $\alpha$ s is disrupted in a tissue-specific manner would be valuable in those investigations, but generation of mice with conditional XL $\alpha$ s ablation could not be accomplished yet (38).

Loss of XL $\alpha$ s imprinting is observed in most patients with PHP-Ib who show broad defects in *GNAS* methylation (23, 24, 39–45). Hypoglycemia is not a typical feature of this disease, but neonatal hypoglycemia has been documented in a PHP-Ib patient who had patUPD20q and, consequently, broad *GNAS* methylation defects (24). It is therefore possible that transient neonatal hypoglycemia occurs more frequently in these patients but is not perceived clinically as a presentation of PHP-Ib. Clinical characterizations of PHP-Ib patients during the early postnatal period will be important to verify whether loss of XL $\alpha$ s imprinting causes hypoglycemia in humans as well.

Unlike hypoglycemia and reduced stomach-to-body weight ratio, the s.c. edema observed around the necks of early postnatal  $\Delta Nesp55^m$  mice was not rescued by the normalization of XL $\alpha$ s expression. This finding is not surprising, because neonatal edema was also observed in several other mouse models in which the maternal *Gas* allele was disrupted (10, 32, 46). Some of these models have normal food intake, including our double-mutant  $\Delta Nesp55^m/Gnasxl^{m+/p-}$  pups, and edema was also noted in utero (47); therefore, insufficient food intake is unlikely to contribute to the edema. Furthermore, 2-d-old  $\Delta Nesp55^m$  pups, which were edematous, did not reveal any overt abnormalities in heart or liver. The mechanism underlying the edema remains to be determined, but it likely involves *Gas* deficiency in a tissue where paternal *Gas* expression is normally silenced.

The hypocalcemia and hyperphosphatemia with elevated PTH in  $\Delta Nesp55^m/Gnasxl^{m+/p-}$  mice is consistent with renal PTH resistance. This finding is also supported by the blunted PTH-induced elevation of urinary cAMP, which is consistent with the reduction in *Gas* mRNA in the renal proximal tubule. However, despite careful isolation and analysis of proximal

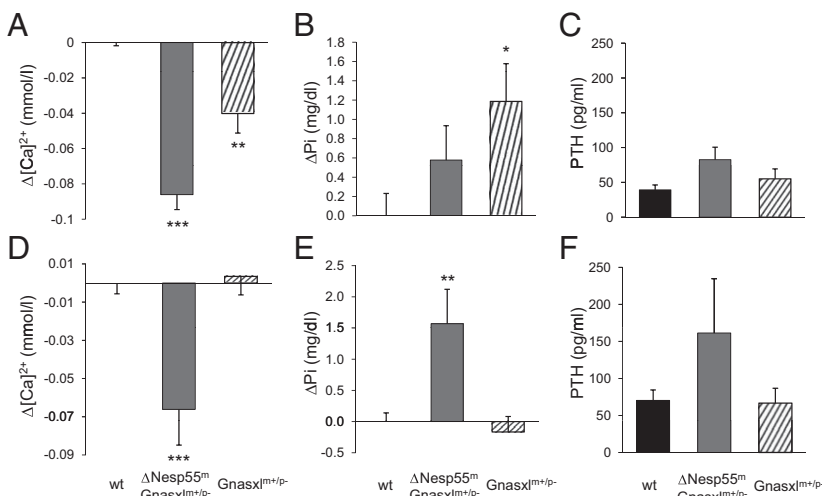


**Fig. 3.** Blood-ionized calcium, phosphorus, and PTH levels in  $\Delta Nesp55^m/Gnasxl^{m+/p-}$  mice and littermates. Blood-ionized calcium ( $\Delta[Ca^{2+}]$ ) and plasma phosphorus ( $\Delta Pi$ ) compared with wild-type (wt) and plasma PTH are presented in 10-d-old (A–C) and adult (D–F) mice. Data are expressed as mean  $\pm$  SEM of 3–8 litters; \* $P < 0.05$ ; \*\* $P < 0.005$ ; \*\*\* $P < 0.0001$  vs. wild type. Ionized calcium levels in wild-type,  $\Delta Nesp55^m/Gnasxl^{m+/p-}$ , and  $Gnasxl^{m+/p-}$  mice were  $1.46 \pm 0.01$  ( $n = 24$ ),  $1.37 \pm 0.01$  ( $n = 18$ ), and  $1.42 \pm 0.01$  ( $n = 23$ ) mmol/L at P10; and  $1.25 \pm 0.01$  ( $n = 30$ ),  $1.18 \pm 0.02$  ( $n = 9$ ), and  $1.25 \pm 0.01$  ( $n = 11$ ) mmol/L in adult, respectively. Plasma phosphorus in wild-type,  $\Delta Nesp55^m/Gnasxl^{m+/p-}$ , and  $Gnasxl^{m+/p-}$  mice were  $10.3 \pm 0.23$  ( $n = 27$ ),  $10.9 \pm 0.36$  ( $n = 20$ ), and  $11.5 \pm 0.39$  ( $n = 10$ ) mg/dL at P10; and  $5.6 \pm 0.1$  ( $n = 16$ ),  $7.1 \pm 0.6$  ( $n = 8$ ), and  $5.4 \pm 0.3$  ( $n = 8$ ) mg/dL in adult, respectively. PTH values of wild-type, double-mutant, and  $Gnasxl^{m+/p-}$  mice were from 20, 20, and 14 mice at P10; and 12, 10, 15 mice in adult, respectively.

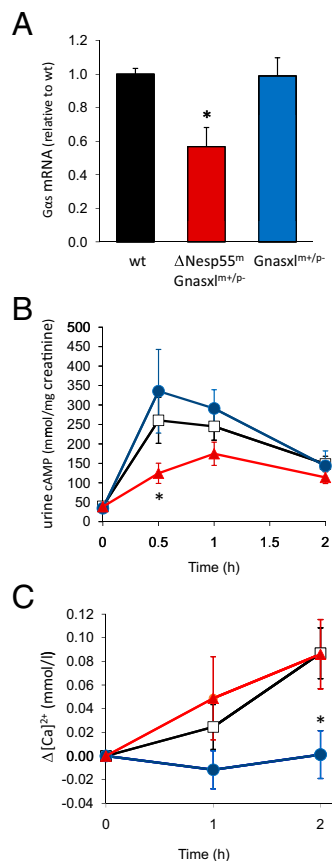


**Fig. 4.**  $G\alpha_s$  mRNA levels in renal proximal tubules of adult  $\Delta Nesp55^{tm}/Gnasxl^{tm+/p-}$  mice and littermates and PTH responsiveness. (A)  $G\alpha_s$  mRNA expression levels were normalized to  $\beta$ -actin mRNA and are shown relative to the levels in wild-type (wt) mice. Tubules were isolated by laser capture microscopy. Data are expressed as mean  $\pm$  SEM of two independent sex-matched littermates of each genotype; \*significantly lower than wild-type ( $P < 0.05$ ). (B and C) PTH-induced urinary cAMP (B) and blood-ionized calcium (C) in wild-type (□),  $\Delta Nesp55^{tm}/Gnasxl^{tm+/p-}$  (▲), and  $Gnasxl^{tm+/p-}$  (●) mice littermates. Mice were injected s.c. with human PTH(1–34), and samples were collected at the indicated times. Data represent mean  $\pm$  SEM of three sex-matched littermates per genotype. \* $P < 0.05$  compared to wild type.

tubules through the use of laser capture microscopy, we found that the reduction in  $G\alpha_s$  levels was only 50%. Thus, the silencing of paternal  $G\alpha_s$  expression may not be complete under normal conditions, and/or this regulatory event may occur only in a subset of proximal tubular cells. Our  $\Delta Nesp55^{tm}/Gnasxl^{tm+/p-}$  mice demonstrated a normal calcemic response to PTH administration, indicating that the actions of PTH on bone are not impaired, as is also true in patients with PHP-Ib (48). This result likely reflects the absence of paternal  $G\alpha_s$  silencing in this tissue (13).

Like  $\Delta Nesp55^{tm}/Gnasxl^{tm+/p-}$  mice, 10-d-old  $Gnasxl^{tm+/p-}$  mice are also hypocalcemic and hyperphosphatemic, suggesting perhaps that  $XL\alpha_s$  contributes to the renal actions of PTH. This explanation would be consistent with previous reports that  $XL\alpha_s$  can mimic  $G\alpha_s$  actions (49, 50), and the absence of hypocalcemia and hyperphosphatemia in adult  $Gnasxl^{tm+/p-}$  mice may indicate that the contribution of  $XL\alpha_s$  protein to mediating the renal effects of PTH may decline with age (50). Conversely, the calcemic response to PTH is blunted in adult  $Gnasxl^{tm+/p-}$  mice (Fig. 4D), suggesting that  $XL\alpha_s$  might still play a role in mediating PTH actions in bone. Consistent with this interpretation,  $XL\alpha_s$  protein expression has been detected in adult mouse osteocytes (51), which are importantly involved in the PTH-

dependent regulation of bone remodeling and calcium homeostasis (52–54).

By generating the  $\Delta Nesp55^{tm}/Gnasxl^{tm+/p-}$  mice, we were able to establish a viable mouse model of AD-PHP-Ib. Although their survival rate was found to be diminished, a substantial number of these double-mutant mice (currently >30) survived to adulthood and had seemingly normal life spans. The mechanisms underlying the pathogenesis of hypocalcemia and hyperphosphatemia resulting from PTH resistance could now be investigated further in the surviving  $\Delta Nesp55^{tm}/Gnasxl^{tm+/p-}$  mice. Furthermore, preweaning lethality of these double-mutant mice may indicate that paternal  $G\alpha_s$  silencing occurs in more tissues than previously recognized or that overexpression of the other paternally expressed  $Gnas$  products—e.g., 1A and *Nespas*—has a negative effect on survival. These questions remain to be addressed.

## Materials and Methods

**Mouse Models.**  $Gnasxl^{tm+/p-}$  and  $\Delta Nesp55^{tm}$  mice were described (30, 31). The  $\Delta Nesp55^{tm}$  mice were crossed into the CD1 strain for more than six generations before mating female  $\Delta Nesp55^{tm}$  mice with male  $Gnasxl^{tm+/p-}$  or  $Gnasxl^{tm+/p+}$  mice, which were also maintained in the CD1 background. Adult mice of the different genotypes were analyzed between 2 and 4 mo of age. These studies were carried out under Institutional Animal Care and Use Committee guidelines and approved by the Massachusetts General Hospital Subcommittee on Research Animal Care.

**Glucose, Insulin, and Corticosterone Analysis.** Glucose was measured from truncal blood by using a glucose strip reader (Precision XceedPro Blood Glucose and  $\beta$ -Ketone Monitoring System; Abbott Laboratories). Truncal blood was furthermore collected into heparinized tubes to generate plasma for additional measurements. Insulin was measured by using the Ultra Sensitive Rat Insulin ELISA Kit (CrystalChem). Corticosterone was measured by using a radioimmunoassay (RIA; MP Biomedical).

**Quantification of Liver Glycogen.** Glycogen content was measured according to Roehrig and Allred (55) after dissolving 20–100 mg of liver tissue in 2 M NaOH. After neutralization (by 2 M HCl), an aliquot of dissolved liver was digested with amyloglucosidase (Sigma) at 55 °C for 15 min. Glucose content was measured by using the Glucose GO Kit (Sigma). Glucose was undetectable in nondigested liver. Values were normalized to the amount of liver protein, determined by the BCA reagent (Pierce). To combine data from different experiments, each value (micrograms of glucose per milligram of protein) was divided by the mean wild-type value obtained in the same experiment.

**Gene Expression Analyses.** Isolation of the renal proximal tubules and extraction of total RNA were as described (50). Total RNA from 2-d-old mouse whole kidney was extracted by using the Qiagen RNeasy Mini kit. Quantitative gene expression analysis for *XL $\alpha_s$*  and *Gus* was performed by TaqMan real-time RT-PCR with  $\beta$ -actin as a reference gene. Calculations were performed by using the accurate cycle threshold method (56). Primers, probes, and conditions are available on request.

**Calcium, Phosphorus, and PTH Measurements.** Blood ionized calcium, plasma phosphorus, and plasma PTH in P10 and adult mice were measured as described (50). In assays to determine PTH responsiveness in vivo, blood and urine were collected from mice before and after s.c. injection of 50 nmol/kg human PTH(1–34). cAMP was quantified by using a RIA (50), and urinary cAMP values were normalized to urinary creatinine measured by using a STANBIO kit.

**Statistical Analyses.** Differences between means were evaluated for statistical significance by using the Student *t* test or, for multiple comparisons among groups of three or more, one-way ANOVA followed by Tukey's post hoc test. The effect of genotype in fasting blood glucose levels was tested by two-way ANOVA.  $\chi^2$  test was used to compare the survival of genotypes at P10.  $P < 0.05$  was considered to be significant. Statistical tests were performed by using GraphPad Prism Software.

**ACKNOWLEDGMENTS.** We thank Drs. Joseph Majzoub and Rong Zhang for help with the corticosterone measurements and Dr. Henry Kronenberg for critically reviewing the manuscript. This work was supported by National Institutes of Health Grants R01DK073911 (to M.B.) and R37DK46718-16 (to

H.J.). Work in the A.P. laboratory is supported by the UK Medical Research Council and the Royal Society. Work in the G.K. laboratory is supported by UK Medical Research Council and the Biotechnology and Biological Sciences

Research Council. S.T. was supported by a Sabbatical Leave Programme grant from the European Society for Paediatric Endocrinology through an educational grant from Lilly USA, LLC.

- Hirasawa R, Feil R (2010) Genomic imprinting and human disease. *Essays Biochem* 48: 187–200.
- Barlow DP (2011) Genomic imprinting: A mammalian epigenetic discovery model. *Annu Rev Genet* 45:379–403.
- Kelsey G (2010) Imprinting on chromosome 20: Tissue-specific imprinting and imprinting mutations in the GNAS locus. *Am J Med Genet C Semin Med Genet* 154C: 377–386.
- Bastepe M (2008) The GNAS locus and pseudohypoparathyroidism. *Adv Exp Med Biol* 626:27–40.
- Peters J, Williamson CM (2008) Control of imprinting at the Gnas cluster. *Adv Exp Med Biol* 626:16–26.
- Kozasa T, Itoh H, Tsukamoto T, Kaziro Y (1988) Isolation and characterization of the human Gs  $\alpha$  gene. *Proc Natl Acad Sci USA* 85:2081–2085.
- Hayward BE, et al. (2001) Imprinting of the G(s)alpha gene GNAS1 in the pathogenesis of acromegaly. *J Clin Invest* 107:R31–R36.
- Mantovani G, Ballare E, Giammona E, Beck-Peccoz P, Spada A (2002) The gsalpha gene: Predominant maternal origin of transcription in human thyroid gland and gonads. *J Clin Endocrinol Metab* 87:4736–4740.
- Liu J, Erlichman B, Weinstein LS (2003) The stimulatory G protein  $\alpha$ -subunit Gs  $\alpha$  is imprinted in human thyroid glands: implications for thyroid function in pseudohypoparathyroidism types 1A and 1B. *J Clin Endocrinol Metab* 88:4336–4341.
- Yu S, et al. (1998) Variable and tissue-specific hormone resistance in heterotrimeric Gs protein  $\alpha$ -subunit (Gsalph) knockout mice is due to tissue-specific imprinting of the gsalph gene. *Proc Natl Acad Sci USA* 95:8715–8720.
- Hayward BE, et al. (1998) The human GNAS1 gene is imprinted and encodes distinct paternally and biallelically expressed G proteins. *Proc Natl Acad Sci USA* 95: 10038–10043.
- Peters J, et al. (1999) A cluster of oppositely imprinted transcripts at the Gnas locus in the distal imprinting region of mouse chromosome 2. *Proc Natl Acad Sci USA* 96: 3830–3835.
- Mantovani G, et al. (2004) Biallelic expression of the Gsalph gene in human bone and adipose tissue. *J Clin Endocrinol Metab* 89:6316–6319.
- Ischia R, et al. (1997) Molecular cloning and characterization of NESP55, a novel chromogranin-like precursor of a peptide with 5-HT1B receptor antagonist activity. *J Biol Chem* 272:11657–11662.
- Hayward BE, Moran V, Strain L, Bonthron DT (1998) Bidirectional imprinting of a single gene: GNAS1 encodes maternally, paternally, and biallelically derived proteins. *Proc Natl Acad Sci USA* 95:15475–15480.
- Kelsey G, et al. (1999) Identification of imprinted loci by methylation-sensitive representational difference analysis: Application to mouse distal chromosome 2. *Genomics* 62:129–138.
- Kehlenbach RH, Matthey J, Huttner WB (1994) XL  $\alpha$  s is a new type of G protein. *Nature* 372:804–809.
- Hayward BE, Bonthron DT (2000) An imprinted antisense transcript at the human GNAS1 locus. *Hum Mol Genet* 9:835–841.
- Wroe SF, et al. (2000) An imprinted transcript, antisense to Nesp, adds complexity to the cluster of imprinted genes at the mouse Gnas locus. *Proc Natl Acad Sci USA* 97: 3342–3346.
- Ishikawa Y, Bianchi C, Nadal-Ginard B, Homcy CJ (1990) Alternative promoter and 5' exon generate a novel G $\alpha$  mRNA. *J Biol Chem* 265:8458–8462.
- Liu J, Yu S, Litman D, Chen W, Weinstein LS (2000) Identification of a methylation imprint mark within the mouse Gnas locus. *Mol Cell Biol* 20:5808–5817.
- Puzhko S, et al. (2011) Parathyroid hormone signaling via G $\alpha$ s is selectively inhibited by an NH(2)-terminally truncated G $\alpha$ s: Implications for pseudohypoparathyroidism. *J Bone Miner Res* 26:2473–2485.
- Liu J, et al. (2000) A GNAS1 imprinting defect in pseudohypoparathyroidism type 1B. *J Clin Invest* 106:1167–1174.
- Bastepe M, Lane AH, Jüppner H (2001) Paternal uniparental isodisomy of chromosome 20q—and the resulting changes in GNAS1 methylation—as a plausible cause of pseudohypoparathyroidism. *Am J Hum Genet* 68:1283–1289.
- Chillambhi S, et al. (2010) Deletion of the noncoding GNAS antisense transcript causes pseudohypoparathyroidism type 1b and biparental defects of GNAS methylation in cis. *J Clin Endocrinol Metab* 95:3993–4002.
- Bastepe M, et al. (2005) Deletion of the NESP55 differentially methylated region causes loss of maternal GNAS imprints and pseudohypoparathyroidism type 1b. *Nat Genet* 37:25–27.
- Linglart A, Gensure RC, Olney RC, Jüppner H, Bastepe M (2005) A novel STX16 deletion in autosomal dominant pseudohypoparathyroidism type 1b redefines the boundaries of a cis-acting imprinting control element of GNAS. *Am J Hum Genet* 76: 804–814.
- Bastepe M, et al. (2003) Autosomal dominant pseudohypoparathyroidism type 1b is associated with a heterozygous microdeletion that likely disrupts a putative imprinting control element of GNAS. *J Clin Invest* 112:1255–1263.
- Chotalia M, et al. (2009) Transcription is required for establishment of germline methylation marks at imprinted genes. *Genes Dev* 23:105–117.
- Fröhlich LF, et al. (2010) Targeted deletion of the Nesp55 DMR defines another Gnas imprinting control region and provides a mouse model of autosomal dominant PHP-1b. *Proc Natl Acad Sci USA* 107:9275–9280.
- Plagge A, et al. (2004) The imprinted signaling protein XL  $\alpha$  s is required for postnatal adaptation to feeding. *Nat Genet* 36:818–826.
- Chen M, et al. (2005) Alternative Gnas gene products have opposite effects on glucose and lipid metabolism. *Proc Natl Acad Sci USA* 102:7386–7391.
- Xie T, et al. (2006) The alternative stimulatory G protein alpha-subunit XLalphas is a critical regulator of energy and glucose metabolism and sympathetic nerve activity in adult mice. *J Biol Chem* 281:18989–18999.
- Abramowitz J, Grenet D, Birnbaumer M, Torres HN, Birnbaumer L (2004) XLalphas, the extra-long form of the alpha-subunit of the Gs G protein, is significantly longer than suspected, and so is its companion Alex. *Proc Natl Acad Sci USA* 101:8366–8371.
- Aydin C, et al. (2009) Extralarge XL(alpha)s (XXL(alpha)s), a variant of stimulatory G protein alpha-subunit (Gs(alpha)), is a distinct, membrane-anchored GNAS product that can mimic Gs(alpha). *Endocrinology* 150:3567–3575.
- Passoli HA, Klemke M, Kehlenbach RH, Wang Y, Huttner WB (2000) Characterization of the extra-large G protein alpha-subunit XLalphas. I. Tissue distribution and subcellular localization. *J Biol Chem* 275:33622–33632.
- Klemke M, Kehlenbach RH, Huttner WB (2001) Two overlapping reading frames in a single exon encode interacting proteins—a novel way of gene usage. *EMBO J* 20: 3849–3860.
- Krechowec SO, et al. (2012) Postnatal changes in the expression pattern of the imprinted signaling protein XL $\alpha$ s underlie the changing phenotype of deficient mice. *PLoS ONE* 7:e29753.
- Linglart A, Bastepe M, Jüppner H (2007) Similar clinical and laboratory findings in patients with symptomatic autosomal dominant and sporadic pseudohypoparathyroidism type 1b despite different epigenetic changes at the GNAS locus. *Clin Endocrinol (Oxf)* 67:822–831.
- Bastepe M, et al. (2011) Paternal uniparental isodisomy of the entire chromosome 20 as a molecular cause of pseudohypoparathyroidism type 1b (PHP-1b). *Bone* 48: 659–662.
- Fernández-Rebollo E, et al.; Spanish PHP Group (2010) New mechanisms involved in paternal 20q disomy associated with pseudohypoparathyroidism. *Eur J Endocrinol* 163:953–962.
- Liu J, Nealon JG, Weinstein LS (2005) Distinct patterns of abnormal GNAS imprinting in familial and sporadic pseudohypoparathyroidism type 1B. *Hum Mol Genet* 14: 95–102.
- Lecumberri B, et al. (2009) Coexistence of two different pseudohypoparathyroidism subtypes (1a and 1b) in the same kindred with independent Gs(alpha) coding mutations and GNAS imprinting defects. *J Med Genet*.
- Mantovani G, et al. (2010) Pseudohypoparathyroidism and GNAS epigenetic defects: Clinical evaluation of albright hereditary osteodystrophy and molecular analysis in 40 patients. *J Clin Endocrinol Metab* 95:651–658.
- Maupetit-Méhouas S, et al. (2011) Quantification of the methylation at the GNAS locus identifies subtypes of sporadic pseudohypoparathyroidism type 1b. *J Med Genet* 48:55–63.
- Skinner JA, Cattanach BM, Peters J (2002) The imprinted oedematous-small mutation on mouse chromosome 2 identifies new roles for Gnas and Gnasxl in development. *Genomics* 80:373–375.
- Williamson CM, et al. (1998) Imprinting of distal mouse chromosome 2 is associated with phenotypic anomalies in utero. *Genet Res* 72:255–265.
- Farfel Z (1999) Pseudohypoparathyroidism-pseudohypoparathyroidism type 1b. *J Bone Miner Res* 14:1016.
- Bastepe M, et al. (2002) Receptor-mediated adenylyl cyclase activation through XLalpha(s), the extra-large variant of the stimulatory G protein alpha-subunit. *Mol Endocrinol* 16:1912–1919.
- Liu Z, et al. (2011) Transgenic overexpression of the extra-large Gs $\alpha$  variant XL $\alpha$ s enhances Gs $\alpha$ -mediated responses in the mouse renal proximal tubule in vivo. *Endocrinology* 152:1222–1233.
- Pignolo RJ, et al. (2011) Heterozygous inactivation of Gnas in adipose-derived mesenchymal progenitor cells enhances osteoblast differentiation and promotes heterotopic ossification. *J Bone Miner Res* 26:2647–2655.
- Powell WF, Jr., et al. (2011) Targeted ablation of the PTH/PTHrP receptor in osteocytes impairs bone structure and homeostatic calcemic responses. *J Endocrinol* 209:21–32.
- Rhee Y, et al. (2011) PTH receptor signaling in osteocytes governs periosteal bone formation and intracortical remodeling. *J Bone Miner Res* 26:1035–1046.
- O'Brien CA, et al. (2008) Control of bone mass and remodeling by PTH receptor signaling in osteocytes. *PLoS ONE* 3:e2942.
- Roehrig KL, Allred JB (1974) Direct enzymatic procedure for the determination of liver glycogen. *Anal Biochem* 58:414–421.
- Livak KJ, Schmittgen TD (2001) Analysis of relative gene expression data using real-time quantitative PCR and the 2(-Delta Delta C(T)) Method. *Methods* 25:402–408.